

RSC Advances



This is an *Accepted Manuscript*, which has been through the Royal Society of Chemistry peer review process and has been accepted for publication.

Accepted Manuscripts are published online shortly after acceptance, before technical editing, formatting and proof reading. Using this free service, authors can make their results available to the community, in citable form, before we publish the edited article. This *Accepted Manuscript* will be replaced by the edited, formatted and paginated article as soon as this is available.

You can find more information about *Accepted Manuscripts* in the [Information for Authors](#).

Please note that technical editing may introduce minor changes to the text and/or graphics, which may alter content. The journal's standard [Terms & Conditions](#) and the [Ethical guidelines](#) still apply. In no event shall the Royal Society of Chemistry be held responsible for any errors or omissions in this *Accepted Manuscript* or any consequences arising from the use of any information it contains.

**Nanoparticle retarded shape relaxation of dispersed droplets in polymer blends:
an understanding from the viewpoint of molecular movement**

Xi-Qiang Liu, Zhen-Yi Sun, Rui-Ying Bao, Wei Yang, Bang-Hu Xie, Ming-Bo Yang*

College of Polymer Science and Engineering, Sichuan University, State Key Laboratory of
Polymer Materials Engineering, Chengdu, 610065, Sichuan, China

Abstract The effect of nano-silica particles on the shape relaxation of the dispersed droplets in polypropylene/polystyrene (PP/PS) blend was investigated. The nano-silica particles were controlled to be distributed in PS phase which presented as the dispersed droplets in the blends. By using an optical microscope equipped with a camera and a hot stage, the shape relaxation of the deformed droplets in the blends after application of a big strain was observed in melt state. The shape relaxation process of PS droplets from highly elongated fibers towards spheres was observed. The nano-silica particles were found to retard the relaxation process of the deformed PS droplets, especially when a particle network was formed. It was showed that the shape relaxation of the droplets was essentially related to the movement of the molecular chains and the relaxation of the oriented chains. These results provide a new understanding on morphology evolution of nanoparticles filled polymer blends based on the retarded movement of molecular chains.

Keywords polymer blends; shape relaxation; molecule movement

Introduction

With the potential to obtain materials with balanced properties, polymer blends have got enormous attention in both industries and academic researches. Factors determining the properties of polymer blends include the properties of consisting components, composition, processing conditions and phase morphology.¹⁻⁴ Immiscible polymer blends often show phase separation and exhibit various morphologies. The dispersed droplet/matrix morphology, with the minor component as dispersed droplets in a continuous phase of the major component, is often observed.⁵⁻⁹ Polymer blends with dispersed droplet/matrix morphology often show high elasticity and a long relaxation time,¹⁰⁻¹³ and the long relaxation time has been considered to correspond to the process in which the deformed droplets recover to its original spherical shape.^{14, 15}

Due to the deformability of liquid interface, the dispersed droplets deform significantly in flow fields during mixing, leading to an increase in interfacial area between components.^{15, 16} The shape of deformed droplets ranges from ellipsoid to highly elongated fibril during processing. After the cessation of flow, the deformed droplets relax back to spherical droplets driven by interfacial tension. Stone et al¹⁷ reported that whether a deformed droplet breaks up is determined by a critical initial elongation ratio which is dependent on the viscosity ratio of the dispersed phase and the continuous phase: for elongation ratios above the critical value the droplets break up into two or multiple daughter droplets during relaxation whereas for elongation ratios below this critical value the deformed droplets simply retract to spheres.

Step strain experiment has been demonstrated to be helpful to understand the mechanism of the droplet deformation and its shape recovery since both processes can be separately detected. When a strain step is applied, a droplet increases in length L and decreases in breadth B . After the step strain, the droplet shape relaxes back to a spherical shape by decreasing L and increasing B . Studies on the droplets with a lower viscosity embedded in a matrix with a higher viscosity¹⁸⁻²¹ showed that: (1) Just after the application of a large strain, a droplet deforms almost affinely to a flat ellipsoid, but the stretch ratio of the major axis of the flat ellipsoid is larger than that predicted from affine deformation; (2) After the cessation of flow, the droplet shape changes from flat ellipsoid to a rod-like shape, a dumbbell, and to an ellipsoid of revolution, and finally back to a sphere; (3) The total recovery time for the deformed droplet increases as the initial radius and the applied strain increase; (4) The orientation angle between the major axis and shear direction does

not change during the shape recovery; (5) The primary driving force for the relaxation of the droplets from the initial flat ellipsoid to the final sphere is the interfacial energy. It was showed that the shape relaxation of the droplets can be divided into two stages. The first stage consists of a shape change towards an ellipsoid without reducing the droplet strain largely in the shear direction, and the second one is the retraction of this ellipsoid accomplished by reducing the droplet strain.^{18, 22} It was also shown that the second stage can be characterized by a single relaxation time, irrespective of the magnitude of the applied shear strain.^{18, 21-23}

The shape relaxation of deformed droplets has been studied mostly in systems consisted of Newtonian components. For systems consisted of viscoelastic components, however, the shape relaxation of droplets has not been paid enough attention. Lerdwijitjarud et al²⁴ reported that droplet viscoelasticity had no influence on the shape relaxation of highly deformed droplets. Tretheway and Leal²⁵ experimentally investigated the deformation and relaxation of a Newtonian drop suspended in a non-Newtonian fluid after a planar extensional flow and concluded that the elastic stress developed at the boundary fundamentally changed the large deformation dynamics and retarded the relaxation process. Cardinaels et al^{22, 26} also showed that droplet viscoelasticity had no influence on the relaxation process whereas matrix viscoelasticity could retard the relaxation process. Yu²⁷ showed that an increase in the elasticity of any constituent of the blends extended the time required to reach equilibrium, both in deformation and relaxation. However, the shape relaxation of droplets in the presence of nano-particles, especially when the nano-particles are distributed in the droplet phase and the droplet viscoelasticity is significantly changed, has not been reported. What should also be pointed out is that most studies concerning the droplet relaxation were performed in confined conditions, in which a spherical droplet was embedded in the matrix polymer and the deformation was generated by subjecting the droplet to a shear flow.¹⁸⁻²³ In some other studies, fibers were first prepared by melt or solution spinning and then embedded into the matrix polymer.²⁸⁻³¹ However, studies adopting both methods show only the shape relaxation of a single droplet in the matrix polymer and cannot reflect the real relaxation process of deformed droplets in immiscible polymer blends. This is because in polymer blends, the droplets will undergo a more complex process when they reform to spherical shape to reduce the interfacial area, during which not only break-up and retraction but also coalescence of the droplets can occur.

In this work, we studied the shape relaxation of droplets, with or without nano-silica particles, in immiscible polymer blends. The objective is to clarify the effect of droplet viscoelasticity on the shape relaxation of droplets in polymer blends. To directly observe the shape relaxation process of the droplets in polymer blends, the morphology evolution of the blends was monitored using an optical microscope equipped with a hot stage and a photographic camera after the application of a large strain. The deformation dynamics of the droplets in the blend, with and without nano-silica particles, was studied. A deeper understanding of the relaxation of the droplets was correlated to its molecular chain movement, which is significantly changed in the presence of nano-silica particles. The blends after mixing were subjected to thermal annealing in the melt state and the morphology formed after annealing for different time was also studied. Our experimental results provided a new understanding on the morphology evolution of inorganic nano-particles filled polymer blends.

Experimental

Materials and sample preparation.

The materials used were two commercial polymers: isotactic polypropylene (PP, T30s, with a weight-average molecular weight of 387, 000 and a polydispersity of 3.6, Kunlun petrochemical co., Ltd., China) and polystyrene (PS, PG-383M, with a weight-average molecular weight of 287, 000 and a polydispersity of 2.34, Zhenjiang chimei chemical co., Ltd., China). The nano-silica particles, hydrophilic Aerosil A200 with an average diameter of 12 nm and a hydroxyl density of 2.5 -OH/nm², were purchased from Evonik Degussa Corporation, Germany.

Prior to processing, PP and PS were dried in a vacuum oven at 80 °C for 12 h. The melt mixing was conducted in a torque rheometer (XSS-300, Shanghai Kechuang Rubber Plastics Machinery Set Ltd., China) at 190 °C. First, PS was mixed with nano-silica particles at 30 rpm for 2 min, and then mixed with PP at 50 rpm for another 5 min. During compounding, a small amount of antioxidant 1010 (0.5 wt% relative to the mass of the whole blend) was added to prevent thermo-oxidative degradation of the polymers. For all the samples, the weight ratio of PP and PS was set as 70/30. The blend samples were marked as 70/30/x%, in which x presents the concentration of nano-silica particles relative to PS phase ranging from 1 to 8wt%. PS composites filled with the same concentration of nano-silica particles (1 to 8wt%) were also prepared under the same processing condition.

Samples for rheological and scanning electron microscopy (SEM) observation were obtained by compression molding. Disk samples of 25 mm diameter and 1.5 mm thickness were molded at a temperature of 190°C under isostatic pressure of 10 MPa for 5 min.

Morphology observation.

The shape relaxation of PS droplets after high degree of deformation was observed on an Olympus BX51 optical microscope (Olympus Co., Tokyo, Japan) equipped with a PixeLINK CCD camera and a hot stage (LINKAM THMS 600). The samples for this real-time observation were obtained on a pressing apparatus schematically described in Fig.1. This apparatus consists of two smooth polished metallic plates between which a polyimide film–sample–polyimide film sandwich is inserted. The difference from the compression molding of the disk samples for rheological measurements is that no mold is used during pressing. Because of this, the materials obtained by melt mixing can be pressed into films which are thin enough to observe the droplets by optical microscope. Furthermore, a big strain can be applied to the sample, leading to that the initial spherical droplets in the blends were highly deformed to fibrillar structure (as schematically shown in Fig. 1). The obtained blend film was sandwiched between two cover glasses fixed on the hot stage and quickly heated to 190°C. Then the morphology evolution of the blend can be observed from the eyepiece of the optical microscope and recorded by the digital camera. In this way, droplets with regular shape were chosen to measure the time dependent sizes (length L and breadth B) using Image-Pro Plus image analysis software.

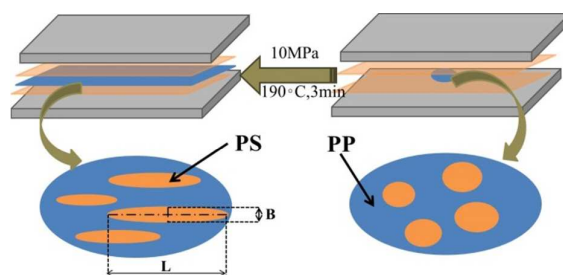


Figure 1 A schematic diagram showing the preparation of film for real-time morphology observation.

Morphology of the blends and the distribution and dispersion of the nano-silica particles were also analyzed using a scanning electron microscopy (SEM, JEOL JSM-5900LV, Japan) at an accelerating voltage of 20 kV. Before SEM observation, the samples were cryo-fractured in liquid nitrogen and then sputtered with gold to avoid charge accumulation.

Rheological measurements.

Rheological measurements were performed on a stress controlled dynamic rheometer (AR2000ex, TA Instruments, USA) at 190°C. A parallel-plate geometry with the plate diameter of 25 mm was used and the gap was set as 1.4 mm. Strain sweep was performed in the strain range of 0.1-100 % at 1Hz to determine the linear viscoelastic region of the samples, and the results showed that the linear viscoelastic region of all the samples was up to 20%. Dynamic frequency sweep was performed from 0.00628 to 628 rad/s within the linear viscoelastic regime. Stress relaxation tests were performed at a given strain of 20% to measure the shear stress $\sigma(t)$ as a function of time and the linear stress relaxation modulus $G(t)$, which was obtained using $G(T) = \sigma(t)/\gamma_0$.

Results and discussion

3.1 Distribution of nano-silica particles

At equilibrium state, the distribution of nano-silica particles in polymer blends is governed by thermodynamics. Normally, the final location of nano-silica particles can be predicted by a wetting parameter (ω_1) proposed by Sumita et al.³²

$$\omega_A = \frac{\gamma_{filler-B} - \gamma_{filler-A}}{\gamma_{A-B}} \quad (1)$$

where $\gamma_{filler-A}$ and $\gamma_{filler-B}$ is the interfacial tension between filler and polymer A and B, respectively; while γ_{A-B} is the interfacial tension between polymer A and polymer B. If $\omega_A > 1$, the filler distributes within polymer A; if $\omega_A < -1$, the filler will locate in the polymer B; if $-1 < \omega_A < 1$, the filler distributes at the interface. Table 1 shows the surface tensions of PP, PS and A200 nano-silica particles at room temperature (23°C) obtained by contact angle measurement of each component with water and diiodomethane. Because the blends were melt mixed at 190°C, it is better to know the surface tension at that temperature. Normally, the surface tension decreases linearly with increasing temperature in the general temperature range (that is, $d\gamma/dT$ is a constant), and $d\gamma/dT$ of macromolecules is smaller than that of small molecules. It is found from literatures that the $d\gamma/dT$ is about 0.05mN/m for PP and PS.³³⁻³⁵ For hydrophilic A200 nano-silica particles, the $d\gamma/dT$ was found to be 0.1 mN/m by Elisa et al.³⁶ Assuming that temperature dependence of the polar and dispersive contribution follows the same law as for the surface tension, the surface tensions of PP, PS and A200 nano-silica particles at 190°C can be obtained,

which are also shown in Table 1.

The interfacial tension of polymer blend or polymer/particle system can be calculated by Wu's equation:³⁷

$$\gamma_{1-2} = \gamma_1 + \gamma_2 - 2\sqrt{\gamma_1^d \gamma_2^d} - 2\sqrt{\gamma_1^p \gamma_2^p} \quad (2)$$

The calculated interfacial tension values of all possible pairs are summarized in Table 2. Taking PP as polymer A, the calculated value of ω_A is -4.9 at 190°C, indicating that the A200 nano-silica particles will distribute in PS phase in PP/PS blend thermodynamically.

Table 1 Surface tension values of PP, PS, nano-silica particles and the nano-silica particle filled PS composite at 23 and 190°C.

Sample	Surface tension at 23°C (mN/m)			Surface tension at 190°C (mN/m)		
	γ	γ^d	γ^p	γ	γ^d	γ^p
A200	77.3	36.5	40.8	60.6	28.6	32
PP	40.3	37.8	2.5	32	29.5	2
PS	51.6	44.6	7	43.3	37.4	5.9
PS/1wt%A200	51.6	42.7	8.9	43.2	35.8	7.48
PS/2wt%A200	51.8	41.9	9.9	43.4	35.1	8.3
PS/4wt%A200	52.2	41.3	10.9	43.9	34.7	9.2
PS/6wt%A200	52.6	41.7	10.9	44.3	35.1	9.2
PS/8wt%A200	52.2	41.1	11.1	43.8	34.5	9.3

Table 2 Interfacial tension values between each possible pair calculated by Equation 2 at 23 and 190°C.

Possible pairs	Interfacial tension (mN/m)	
	23°C	190°C
PP/A200	23.1	18
PS/A200	14.4	11
PP/PS	1.4	1.4
PP/(PS/1wt%A200)	2.1	2.5
PP/(PS/2wt%A200)	2.	2.9
PP/(PS/4wt%A200)	3	3.3
PP/(PS/6wt%A200)	3	3.3
PP/(PS/8wt%A200)	3.1	3.4

To prevent the migration of the nano-silica particles during processing, we adopted a two-step compounding method, that is, mixing nano-silica particles with PS first and then PP was introduced. Figure 2a shows the morphology of 8wt% A200 nano-silica particle (relative to the weight of PS phase) filled PP/PS 70/30 blend. It is found that the blend shows a typical dispersed droplets/ matrix morphology with the minor PS phase being spherical or elliptical droplets dispersed in PP matrix. Fig.2b presents the magnified micrograph of the circled area in Fig.2a, where both the matrix PP phase and the dispersed PS phase are included. In matrix PP phase, the surface is smooth and almost no particles are found. In the dispersed PS phase, the surface is rough and covered by a lot of small bumps, which are silica particles (as the arrow pointed). The SEM micrographs demonstrate that the nano-silica particles are almost totally distributed in the dispersed PS droplets.

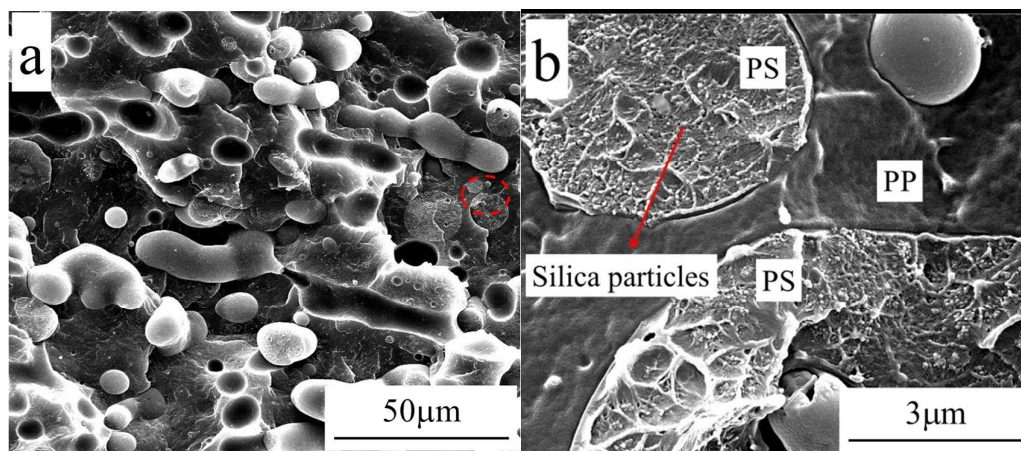


Figure 2 Morphology of 8wt% A200 nano-silica particle (relative to the weight of PS phase) filled PP/PS 70/30 blend. Image b is the magnified image of image a.

3.2 Shape relaxation of PS droplets in the blend

Fig.3 shows the morphology evolution of PP/PS blend at 190°C after the application of a big strain using the pressing apparatus. The blend initially presents a fibrillar structure, indicating that PS droplets deform significantly after the application of strain. During annealing at 190°C, the shapes of the droplets show an relaxation process from highly deformed fibers to spheres. The relaxation patterns and the relaxation time of deformed droplets greatly depend on the deformation degree of the droplets. For slightly deformed droplets with an initial flat ellipsoid shape, the droplets change their shape from an ellipsoid to a rod-like shape and to a dumbbell, an ellipsoid of revolution, and finally back to a sphere. For highly deformed droplets with a fiber shape, breakup

happens at the early stage of melt annealing, leading to multiple daughter droplets with less deformation. The droplets formed due to the breakup of highly deformed droplets will continue to retract into spheres. The relaxation time of the droplets increases with the deformation degree and most droplets can retract into spheres within 30 minutes. However, it is found that some highly deformed droplets are connected with each other. In this case, the formed droplets present irregular shapes rather than ellipsoid when breakup occurs and the relaxation of these irregular droplets will become slower.



Figure 3 Morphology development of pure PP/PS 70/30 blend observed via an optical microscope in real time during annealing at 190°C

Fig.4 shows the morphology evolution of PP/PS blends at 190°C with 4wt% nano-silica particles (relative to the mass of PS phase) in PS droplets. The shape relaxation process is similar to that of pure blend. However, the relaxation time required for a deformed droplet is significantly increased. Many deformed droplets can still be seen even after 2 hours of melt annealing at 190°C. The results clearly indicate that the incorporation of nano-silica particles retard the shape relaxation of PS droplets. The retardance effect of nano-silica particles is greatly dependent on their concentration. With 2wt% particles (relative to the mass of PS phase), the shape relaxation of

PS droplets is slightly slowed while when 8wt% particles (relative to the mass of PS phase) are filled, the relaxation process is significantly retarded. (The morphology evolution of PP/PS blends at 190°C with 2 and 8wt% nano-silica particles (relative to the mass of PS phase) in PS droplets is given in supported information.)

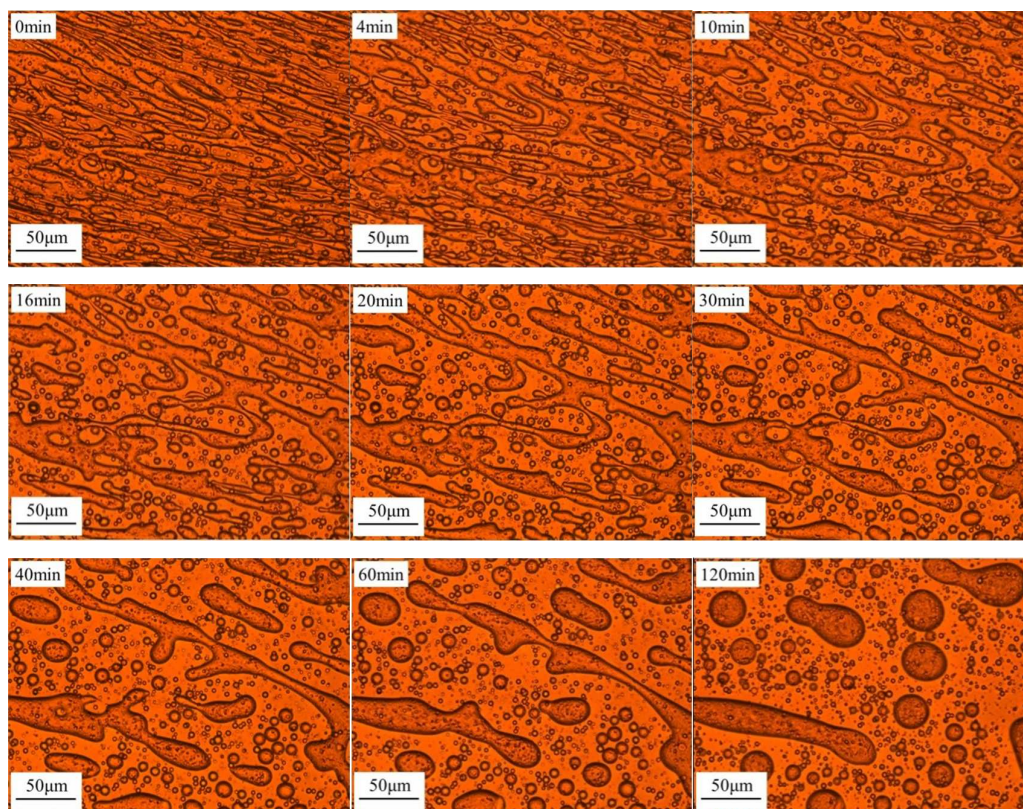


Figure 4 Morphology development of 4wt% A200 nano-silica particle (relative to the weight of PS phase) filled PP/PS 70/30 blend during annealing at 190°C

To more directly present the effect of the nano-silica particles on the shape relaxation process of the droplets, we tracked some PS droplets in each blend and recorded the dimension change during annealing. Fig.5 shows the time dependence of the length and the breadth of PS droplets, which are all normalized by the diameters of the final spheres d_0 . For the blend with 8wt% nano-silica particles (relative to the weight of PS phase), the PS droplets cannot retract into a sphere during annealing and the d_0 is calculated based on the final spheres having the same volume with the initial ellipsoid droplet. According to Fig.5, the curves of the blends are similar except for the blend with 8wt% nano-silica particles (relative to the weight of PS phase). Initially, the L/d_0 decreases quickly due to breakup of the droplets, but the value of B/d_0 does not change for several hundreds of seconds. Then both L/d_0 and B/d_0 almost change linearly with annealing time

in the double logarithm curve. In the end, L/d_0 and B/d_0 approach to unity indicating that the droplets have nearly retracted into spheres. It is also found that the relaxation time of PS droplets with almost identical length and width increases with the incorporation of nano-silica particles. This inhibition effect of particles toward shape relaxation of droplets is much more significant at high concentration of particles.

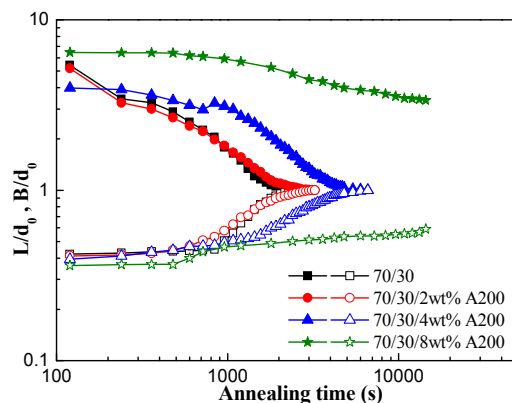


Fig.5 Time dependence of the normalized droplet length and width, L/d_0 and B/d_0 for PS droplets

3.3 Relaxation time of PS droplets

For highly deformed droplets, the shape relaxation is commonly studied by means of the evolution of the Hencky strain Γ ^{18, 22} and Taylor's extent of deformation D ^{38, 39} which are defined as:

$$\Gamma = \ln(L/d_0) \quad (3)$$

$$D = (L - B)/(L + B) \quad (4)$$

in which the value of D changes from 1 (if the initial droplet is infinitely extended) to 0 (sphere) during relaxation. If the shape recovery is a relaxation process with a single relaxation time, τ , Γ and D can be expressed as:

$$\Gamma = \Gamma_0 \exp(-t/\tau) \quad (5)$$

$$D = D_0 \exp(-t/\tau) \quad (6)$$

and plots of $\log\Gamma$ and $\log D$ vs t would give straight lines, from which the characteristic relaxation time can be obtained. Fig.6a shows the plot of $\log[\ln(L/d_0)]$ vs t and Fig.6b shows the plot of $\log[(L - B)/(L + B)]$ vs t for PS droplets in each blend, respectively. It is found that both plots show similar trends and the relaxation curves can generally be divided into two stages: an initial relatively slow decay followed by a faster decay. It is reported that during the first stage, the

droplet just changes its shape towards an ellipsoid without largely reducing the droplet strain. During the second stage of the relaxation, where the droplet shape is an ellipsoid of revolution, reduction of the interfacial area is accomplished by reducing the droplet strain. Reduction of the droplet strain during the second stage can be expressed by a characteristic time constant which does not depend on the magnitude of the applied strain. This characteristic time constant is nearly equal to the relaxation time of the dispersed phase in the blend for linear viscoelasticity predicted by the emulsion model of Palierne.¹¹ By linearly fitting the curves with time in the second stage, the characteristic relaxation times, which are independent of the initial deformation and the time after the application strain, of PS droplets in each blend are obtained and summarized in Table 3.

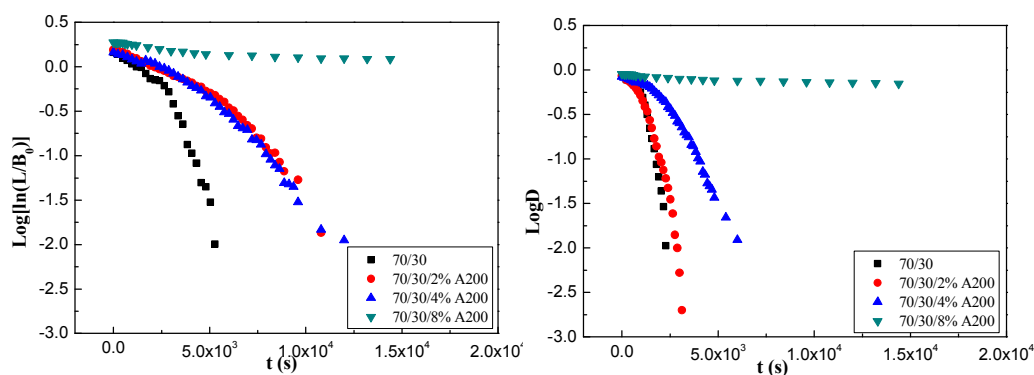


Fig.6 Time dependence of (a) $\log[\ln(L/d_0)]$ and (b) $\log[(L - B)/(L + B)]$ for various samples

As shown in Table 3, the characteristic relaxation time, obtained from the plots of both Γ and D , increases with the incorporation of nano-silica particles, indicating a retardance effect of particles towards the relaxation of the droplets. However, the relaxation time increases but not linearly with the particle concentration. For the blend with a low concentration of particles, the relaxation time only increases moderately while for 8wt% particles filled blend, a huge relaxation time is obtained. This corresponds well with the results of real-time observation where the PS droplets only slightly retracted even after annealing for 4h.

Table 3 Droplet relaxation times according to Equation 5 and 6 in each blend.

	70/30	70/30/2%A200	70/30/4%A200	70/30/8%A200
τ_{Γ} (s)	702	1723	2065	82924
τ_D (s)	339	586	1059	104400

3.4 Relationship between droplet relaxation and molecular chains relaxation

Rheology has been proved to be a powerful tool to probe the structure and structural evolution in materials. Fig.7 shows the storage modulus (G') and complex viscosity (η^*) as a function of

frequency for PP, PS and nano-silica particle filled PS composites at 190°C. At low frequencies, homopolymer chains can be fully relaxed and usually exhibit a characteristic terminal behavior with $G' \propto \omega^2$.⁴⁰⁻⁴² Here, pure PP and PS melt exhibit approximately a terminal-like behavior at low frequencies. With increasing concentration of nano-silica particles, the storage modulus of PS composites increases remarkably at low frequencies, exhibiting a reinforcing effect. At the same time, the frequency dependence of G' at low frequencies becomes weaker evidenced by the reduced slopes of the modulus curves. For 8wt% nano-silica filled PS composite, a frequency independent G' plateau is observed at low frequencies, indicates a transition from liquid-like to solid-like viscoelastic behavior.⁴³⁻⁴⁶ For the complex viscosity, as shown in Fig.7b, pure PP and PS show a Newtonian region at low frequencies and a shear-thinning region at higher frequencies. With increasing particle concentration, the Newtonian region gradually disappears and at a nano-silica concentration of 8wt%, the melt shows shear-thinning behavior in the whole frequency range, which indicates the existence of a yield stress.⁴⁶⁻⁴⁹ The development of a finite yield stress, accompanied by the development of a G' plateau, is often associated with the formation a percolated particle network structure.⁴³⁻⁴⁹

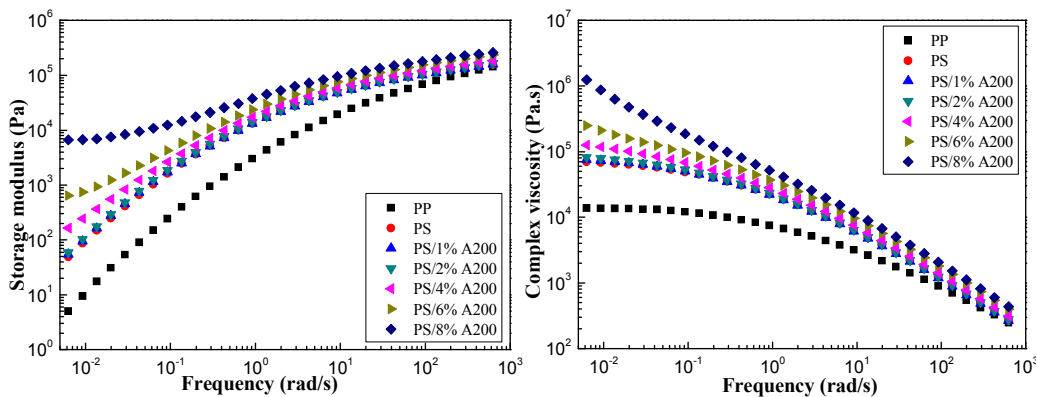


Fig.7. (a) Storage modulus, (b) complex viscosity as a function of frequency for PP, PS and nano-silica particle filled PS composites.

Shear thinning and G' plateau are the result of an increase in relaxation time with respect to pure polymer. This can be revealed more evidently in the weighted relaxation time spectra (the $H(\lambda)*\lambda \sim \lambda$ curve, in which $H(\lambda)$ is the continuous relaxation converted by dynamic properties and λ is the relaxation time⁵⁰) provided in Fig. 8. PP and PS show a relaxation peak at 1.96 s and 4.04 s, respectively. With increasing nano-silica particle concentration, the relaxation peak of PS phase shifts towards the direction with longer time. At the nano-silica concentration of 8wt%, the

relaxation peak cannot be detected in the measured time scale, indicating a much longer relaxation time. This definitely indicates that the relaxation of PS chains is retarded, especially when a particle network structure is formed.

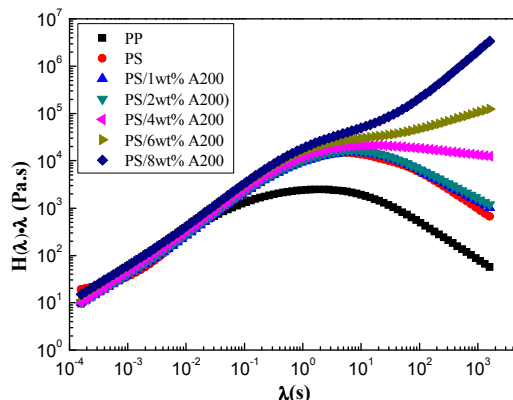


Fig. 8. Weighted relaxation time spectra for PP, PS and nano-silica particle filled PS composites.

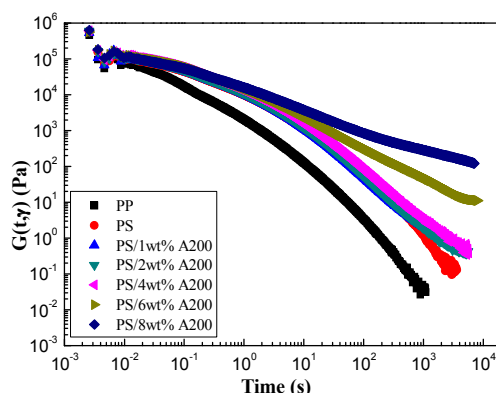


Fig.9 Stress relaxation modulus $G(t,\gamma)$ as a function of time for PP, PS and nano-silica particles filled PS composites at a temperature of 190°C

Stress relaxation behavior is also measured to reveal the effect of nano-silica particles on the relaxation of the PS composites. As is known, an internal stress develops upon the application of a large strain and the molecular chains will be oriented in some degree. To decrease or eliminate the internal stress, molecular chains will move or rearrange to reach an equilibrium state and this process is highly dependent on the entanglement state of molecular chains and temperature. With increasing flexibility of the chains or elevating temperature, the relaxation time becomes shorter. As shown in Fig.9, pure components of PP and PS present a rapid one-step relaxation and the relaxation time of PS is much longer than that of PP, showing a relatively poor mobility of PS chains due to the existence of benzene groups. With increasing particle concentration in PS phase, the slope of the relaxation curve decreases, leading to that the time required of $G(\gamma, t)$ to decline to

a fixed value increases, i.e. the relaxation becomes slower. This phenomenon is more significant for 8wt% particle filled PS composite, where the $G(\gamma, t)$ shows a linear decline in the whole time range with a much smaller slope. When nano-silica particles are filled, even though the internal stress still exists, the internal friction is increased and the mobility of molecular chains becomes suppressed. As a result, the stress relaxation becomes slow. With the formation of a particle network, a huge friction resistance produces and the mobility of the molecular chains is significantly suppressed, leading to that the stress relaxation is significantly slowed.

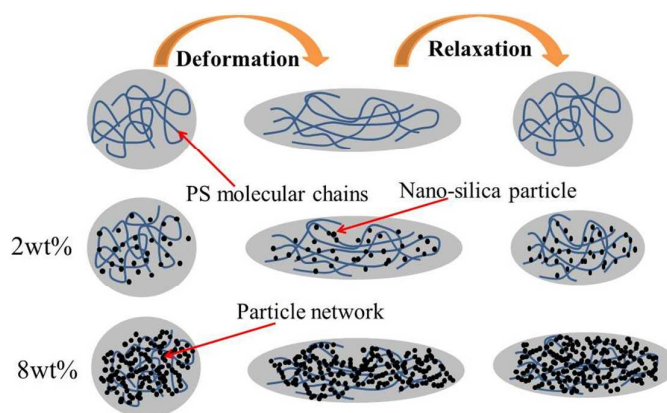


Fig.10 Schematic diagram of retarded shape relaxation of dispersed droplets filled with nano-silica particles.

Fig.10 schematically shows the retardance effect of nano-silica particles on the shape relaxation of PS droplets in the blend. Upon the application of a strain to the blend, PS droplets deform and form fibrillar droplets. PS molecular chains also move along the direction of the applied strain and the entangled state of molecular chains is changed, more precisely, the molecular chains are oriented compulsively. After the application of the strain, the droplets will relax from the stretched shape to spherical shape to decrease the interfacial energy, and at the same time, the molecular chains move back to original position and the oriented chains relax to original entangled state. Both processes are highly dependent on the mobility of molecular chains. When nano-silica particles are filled, molecular chains are absorbed on the particle surface, which increases the frictions when the chains move. So the movement of the molecular chains and the relaxation of the oriented chains become difficult and the shape relaxation of the deformed droplets becomes slow. With the formation of a particle network, the molecular chains are highly trammled. Upon the application of a strain, the particle network is also deformed accompanying the deformation of the droplets. What differs from the deformation of droplets is that the deformation of particle

network only means that the location of particles is changed, however, the particles are still in an equilibrium state and no internal stress exists in the network. As a result, the deformed particle network cannot recover itself. To relax, the molecular chains must drive the particle network to deform, which will consume a large amount of energy. As a result, the relaxation of molecular chains is significantly slowed and the shape relaxation of the droplets is significantly retarded.

3.5 Morphology compatibilizing effect of nanoparticles

In recent years, the concept of compatibilization by using inorganic nanoparticles has been put forward and widely utilized. The compatibilizing effect of inorganic nanoparticles is often evidenced by the morphology refinement of polymer blends such as the reduction of the size of the dispersed droplets,^{36, 50-63} the improvement of interfacial interaction⁵⁶⁻⁶⁰ and the stabilization of blend morphology.⁶¹⁻⁶⁴ The morphology compatibilizing mechanism of inorganic nanoparticles is often attributed to the reduction of the interfacial tension due to the selective location of the particles at the interface.^{36, 50-59} Furthermore, mechanisms including viscosity increase of the phases^{65, 66} and the inhibition of coalescence with the presence of a solid barrier around the droplets⁶¹⁻⁶⁵ are also proposed.

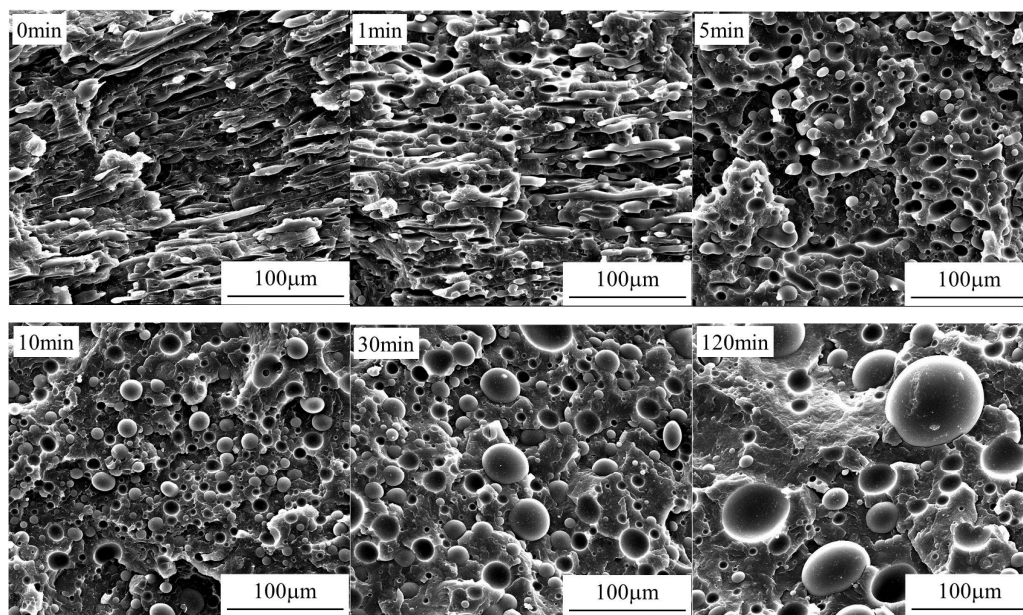


Fig.11 Morphology evolution of pure PP/PS 70/30 blend annealed at 190°C for different time.

We also observe the morphology compatibilizing effect of the nano-silica particles in PP/PS blends. Fig. 11 and Fig.12 show the morphology evolution of pure PP/PS blend and the blend with 8wt% nano-silica particles (relative to the weight of PS phase) filled in PS phase after annealing

for different time, respectively. It is found that both blends, just after processing, present a fibrillar structure with the PS droplets being highly stretched. By annealing in the melt state, the stretched PS droplets quickly retract into spherical droplets in a time scale less than 10min for pure blend. After that, serious coarsening by coalescence of the spherical droplets happens, leading to a huge increase in the droplet size. For the blend with 8wt% particles filled in PS droplets, however, the retraction of the stretched PS droplets to spherical droplets is very slow, the reason of which has been expounded previously. Due to the poor mobility of the stretched droplets, the coalescence of the droplets is greatly suppressed. As a result of the slow retraction and slight coalescence of PS droplets, the size increase of the droplets is very limited. According to Tab.2, the interfacial tensions between PP and PS do not decrease after the incorporation of nano-silica particles in PS phase, on the contrary, they are slightly increased. So the reduction of the droplet size is achieved by slowing the shape relaxation and coalescence process of the deformed droplets. These results also agree with the reports of Okubo⁶⁷ and Vignati and Piazza⁶⁸, who demonstrated that the interfacial tension between the two liquids of the emulsion was unaffected by particles. In essence, the morphology compatibilizing effect of inorganic nanoparticles is a result of the retarded movement of molecular chains rather than the reduction of interfacial tension.

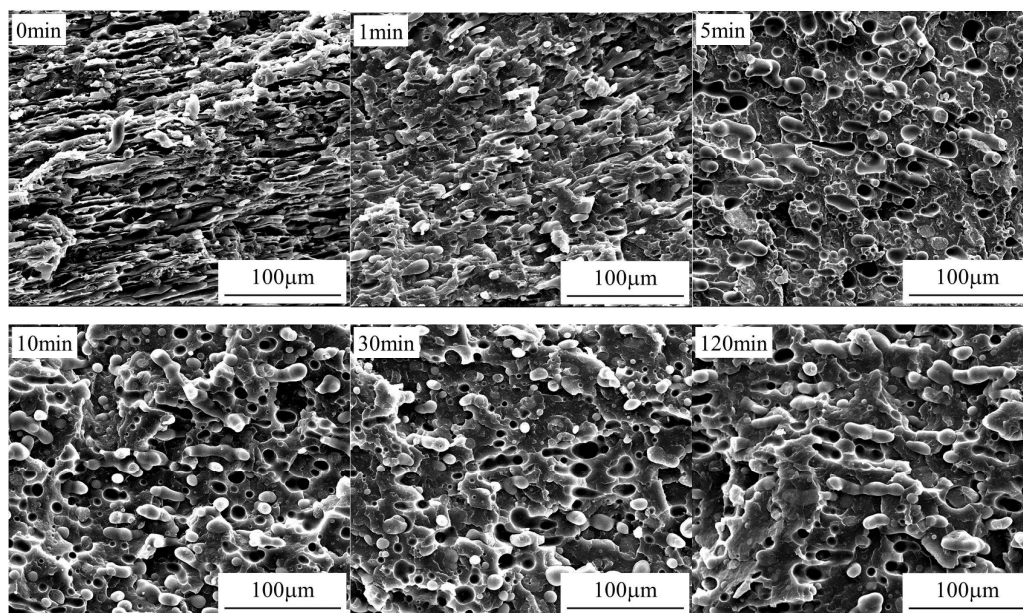


Fig.11 Morphology evolution of 8wt% A200 nano-silica particle (relative to the weight of PS phase) filled PP/PS 70/30 blend annealed at 190°C for different time.

4 Conclusions

The effect of nano-silica particles on the shape relaxation of deformed droplets in PP/PS blend is studied in detail. With the selective distribution of the particles in PS droplets, the shape relaxation of PS droplets from fibrillar structure towards spheres is retarded. The relaxation process is more significantly retarded when the particles form a network structure in PS phase. It is showed that the shape relaxation of the deformed droplets is essentially related to the movement of the molecular chains and the relaxation of the oriented chains. When nano-silica particles are introduced, the mobility of molecular chains is decreased due to the increased friction, which leads to that the relaxation of molecular chains becomes slow. With a particle network formed, the movement of the molecular chains and the relaxation of the oriented chains become even slower since the molecular chains must drive the particle network to deform, which will consume large amounts of energy. As a result, the shape relaxation of the droplets is significantly retarded. Based on this research, it is considered that the morphology compatibilizing mechanism of nanoparticles in polymer blends is achieved by retarding the movement of molecular chains rather than reducing the interfacial tension.

Acknowledgement

The authors are grateful to the National Natural Science Foundation of China (Grant Nos. 21374065 and 51121001), Major State Basic Research Development Program of China (973 program) (2012CB025902), Fundamental Research Funds for the Central Universities (Grant No. 2011SCU04A03) and the Innovation Team Program of Science & Technology Department of Sichuan Province (Grant 2013TD0013). Mr. Chao-liang Zhang, working at the State Key Laboratory of Oral Medicine of China, was also acknowledged for his kind help in FE-SEM observations.

References

- 1 J. W. Barlow and D. R. Paul, *Polym. Eng. Sci.*, 1984, **24**, 525-534.
- 2 C. W. Macosko, P. Guégan and A. K. Khandpur, *Macromolecules*, 1996, **29**, 5590-5598.
- 3 R. B. Grubbs, J. M. Dean, M. E. Broz and F. S. Bates, *Macromolecules*, 2000, **33**, 9522-9534.
- 4 H. Wu, Z. H. Su, and A. Takahara, *RSC Adv.*, 2012, **23**, 8707-8712.
- 5 K. Binder and D. Stauffer, *Phys. Rev. Lett.*, 1974, **33**, 1006-1009.

- 6 I. S. Polios, M. Soliman, C. Lee, S. P. Gido, K. Schmidt-Rohr, and H. H. Winter, *Macromolecules*, 1997, **30**, 4470-4480.
- 7 I. Vinckier and H. M. Laun, *Rheol. Acta.*, 1999, **38**, 274-286.
- 8 J. M. Li and B. D. Favis, *Macromolecules*, 2002, **35**, 2005-2016.
- 9 X. Q. Liu, W. Yang, B. H. Xie and M. B. Yang, *Mater. Design.*, 2012, **34**, 355-362.
- 10 H. K. Chuang and C. D. Han, *J. Appl. Polym. Sci.*, 1984, **29**, 2205-2229.
- 11 J. F. Palierne, *Rheol. Acta.*, 1990, **129**, 204-214.
- 12 D. Graebling, R. Muller and J. F. Palierne, *Macromolecules*, 1993, **26**, 320-329.
- 13 S. Maeda, and E. Kamei, *J. Soc. Rheol. Jpn.*, 1994, **22**, 145-154.
- 14 D. F. Wu, L. J. Yuan, E. Laredo, M. Zhang and W. D. Zhou, *Ind. Eng. Chem. Res.*, 2012, **51**, 2290-2298.
- 15 P. H. P. Macaúbas, H. Kawamoto, M. Takahashi, K. Okamoto and T. Takigawa, *Rheol. Acta.*, 2007, **46**, 921-932.
- 16 L. Levitt and C. W. Macosko, *Polym. Eng. Sci.*, 1996, **36**, 1647-1655.
- 17 H. A. Stone, B. J. Bentley and L. G. Leal, *J. Fluid. Mech.*, 1986, **173**, 131-158.
- 18 H. Yamane, M. Takahashi, R. Hayashi and K. Okamoto, *J. Rheol.*, 1998, **42**, 566-580.
- 19 K. Okamoto, M. Takahashi, H. Yamane, H. Kashiwara, H. Watanabe and T. Masuda, *J. Rheol.*, 1999, **43**, 951-965.
- 20 R. Hayashi, M. Takahashi, H. Yamane, H. Jinnai and H. Watanabe, *Polymer*, 2001, **42**, 757-764.
- 21 R. Hayashi, M. Takahashi, T. Kajihara and H. Yaman, *J. Rheol.*, 2001, **45**, 627-639.
- 22 R. Cardinaels and P. Moldenaers, *J. Polym. Sci., Part B: Polym. Phys.*, 2010, **48**, 1372-1379.
- 23 S. Assighaou and L. Benyahia, *Phys. Rev. E.*, 2008, **77**, 036305.
- 24 W. Lerdwijitjarud, R. G. Larson, A. Sirivat and M. J. Solomon, *J. Rheol.*, 2003, **47**, 37-58.
- 25 D. C. Tretheway and L. G. Leal, *J. Non-Newtonian Fluid Mech.*, 2001, **99**, 81-108.
- 26 R. Cardinaels and P. Moldenaers, *Rheol. Acta.*, 2010, **49**, 941-951.
- 27 W. Yu, M. Bousmina, C. X. Zhou and C. L. Tucker, *J. Rheol.*, 2004, **48**, 417-438.
- 28 C. J. Carriere, A. Cohen and C. B. Arends, *J. Rheol.*, 1989, **33**, 681-689.
- 29 M. Tjahjadi, J. M. Ottino and H. A. Stone, *AIChE. J.*, 1994, **40**, 385-394.
- 30 H. Y. Mo, C. X. Zhou and Wei Yu, *J. Non-Newtonian Fluid Mech.* 2000, **91**, 221-232.
- 31 G. Palmer and R. Nicole, *Polymer*, 2005, **46**, 8169-8177.
- 32 M. Sumita, K. Sakata, S. Asai, K. Miyasaka and H. Nakagawa, *Polym. Bull.*, 1991, **25**, 265-271.
- 33 S. Wu, *J. Colloid Interface Sci.*, 1969, **31**, 153-161.
- 34 S. Wu, *J. Polym. Sci.*, 1971, **C34**, 19-30.
- 35 S. Wu, *J. Phys. Chem.*, 1968, **72**, 2013.
- 36 L. Elias, F. Fenouillot, J. C. Majeste and P. Cassagnau, *Polymer*, 2007, **48**, 6029-6040.
- 37 S. Wu, *Polymer Interface and Adhesion*. Marcel Dekker, New York, 1982, p534.
- 38 G. I. Taylor, *Proc. R. Soc. London Ser. A.*, 1932, **138**, 41-48.

- 39 G. I. Taylor, Proc. R. Soc. London Ser. A., 1934, **146**, 501-523.
- 40 D.S. Bangarusampath, H. Ruckdäschel, V. Altstädt, J. K.W. Sandler, D. Garray and M. S. P. Shaffer, Polymer, 2009, **50**, 5803-5811.
- 41 R. V. Krishnamoorti, R. V. Vaia and G. P. Giannelis, Chem. Mater., 1996, **8**, 1728-1734.
- 42 C. A. Mitchell, J. L. Bahr, S. Arepalli, J. M. Tour and R. Krishnamoorti, Macromolecules, 2002, **35**, 8825-8830.
- 43 N. S. Enikolopyan, M. L. Fridman, I. O. Stalnova and V. L. Popov, Adv. Polym. Sci., 1990, **96**, 1-67.
- 44 P. Pötschke, T. D. Fornes and D. R. Paul, Polymer, 2002; **43**, 3247-55.
- 45 N. Jouault, P. Vallat, F. Dalmas, S. Said, J. Jestin and F. Boué, Macromolecules, 2009, **42**, 2031-2040.
- 46 Y. H. Song, Q. Zheng, Polymer, 2010, **51**, 3262-3268.
- 47 R. V. Krishnamoorti, R. A. Vaia and E. P. Giannelis, Chem. Mater., 1996, **8**, 1728-1734.
- 48 C. A. Mitchell and R. Krishnamoorti, Macromolecules, 2007, **40**, 1538-1545.
- 49 P. Pötschke, M. Abdel-Goad, I. Alig, S. Dudkin and D. Lellinger, Polymer, 2004, **45**, 8863-8870.
- 50 V. Shaayegan, P. Wood-Adams and N. R. Demarquette, J. Rheol., 2012, **56**, 1039-1056.
- 51 Q. Zhang, H. Yang and Q. Fu, Polymer, 2004, **45**, 1913-1922.
- 52 Y. Liu and M. Kontopoulou, Polymer, 2006, **47**, 7731-7739.
- 53 H. Yang, X. Q. Zhang, C. Qu, B. Li, L. J. Zhang, Q. Zhang and Q. Fu, Polymer, 2007, **48**, 860-869.
- 54 F. Laoutid, E. Estrada, R. M. Michell, L. Bonnaud, A. J. Müller and P. Dubois, Polymer, 2013, **54**, 3982-3993.
- 55 Z. Hrnjak-Murgic, Z. Jelcic, V. Kovacevic, M. Mlimac-Misak and J. Jelenci, Macromol. Mater. Eng., 2002, **287**, 684-692.
- 56 J. S. Hong, H. Namkung, K. H. Ahn, S. J. Lee SJ and C. Kim, Polymer, 2006, **47**, 3967-3975.
- 57 M. Y. Gelfer, H. H. Song, L. Z. Liu, B. S. Hsiao, B. Chu, M. Rafailovich, M.Y. Si and V. Zaitsev, J. Polym. Sci., Part B: Polym. Phys., 2003, **41**, 44-54.
- 58 Y. Wang, Q. Zhang and Q. Fu, Macromol. Rapid. Commun., 2003, **24**, 231-235.
- 59 S. Nagarkar and S. S. Velankara, J. Rheol., 2013, **57**, 901-926.
- 60 S. B. Ye, Y. M. Cao, J. C. Feng and P. Y. Wu, RSC Adv, 2013, **21**, 7987-7995.
- 61 W. Tong, Y. J. Huang, C. L. Liu, X. L. Chen, Q. Yang and G. X. Li, Colloid. Polym. Sci., 2010, **288**, 753-760.
- 62 J. Vermant, G. Cioccolo, K. G. Nai and P. Moldenaers, Rheol. Acta., 2004, **43**, 529-538.
- 63 M. Si, T. Araki, H. Ade, A. L. D. Kilcoyne, R. Fisher, J. C. Sokolov and M. H. Rafailovich,

Macromolecules, 2006, **39**, 4793-4801.

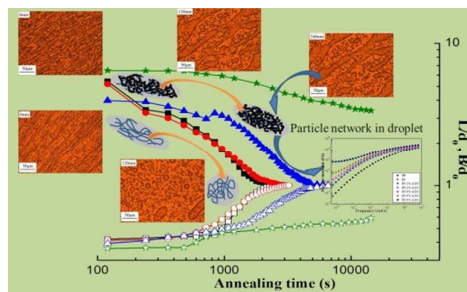
64 F. Gubbels, S. Blacher, E. Vanlathem, R. Jérôme, J. R. Deltour, O. F. Brouers and P. Teyssibé, Macromolecules, 1996, **28**, 1559-1566.

65 D. Wu, L. Wu, M. Zhang, W. Zhou and Y. Zhang, J. Polym. Sci., Part B: Polym. Phys., 2008, **46**, 1265-1279.

66 L. Zhang, K. C. Tam, L. H. Gan, C. Y. Yue, Y. C. Lam, X and Hu, J. Appl. Polym. Sci., 2003, **87**, 1484-1492.

67 T. Okubo, J. Colloid. Interface. Sci., 1995, **171**, 55-62.

68 E. Vignati and R. Piazza, Langmuir, 2003, **19**, 6650-6656.



Nanoparticle network in dispersed droplets of polymer blends retards the shape relaxation of droplets by inhibiting molecular movement.